

Topological superconductivity and Majorana bound states at the LaAlO₃/SrTiO₃ interface

N. Mohanta^{1,*} and A. Taraphder^{1,2}

¹*Department of Physics, Indian Institute of Technology Kharagpur, W.B. 721302, India*

²*Centre for Theoretical Studies, Indian Institute of Technology Kharagpur, W.B. 721302, India*

The interface between two band insulators LaAlO₃ and SrTiO₃ exhibits low-temperature superconductivity coexisting with an in-plane ferromagnetic order. We show that topological superconductivity hosting Majorana bound states can be induced at the interface by applying a magnetic field perpendicular to the interface. We find that the dephasing effect of the in-plane magnetization on the topological superconducting state can be overcome by tuning a gate-voltage. We analyze the vortex-core excitations showing the zero-energy Majorana bound states and the effect of non-magnetic disorder on them. Finally, we propose an experimental geometry where such topological excitations can be realized.

PACS numbers: 74.20.Rp, 03.65.Vf, 74.62.Dh

I. INTRODUCTION

Majorana fermion, which often arises as a quasi-particle excitation in condensed matter systems, is being studied intensively due to its indispensable utility in defect-free topological quantum computation [1]. The Majorana bound state (MBS) naturally exists in spin-triplet chiral p -wave superconductivity in superfluid He³ (A-phase) [2] and Sr₂RuO₄ [3] and in the fractional quantum Hall state at 5/2 filling [4]. Also, there have been several proposals of experimentally feasible systems that host MBS such as quantum wire coupled to s -wave superconductor [5], semiconductor-superconductor heterostructure [6, 7], proximity-induced superconductor at the surface of topological insulator [8], 2DEG at semiconducting quantum well [9], and the more promising Al-InSb nanowire topological superconductor [10]. Also there is a trend to realize topological orders in fermionic s -wave superfluids of ultracold atoms in optical lattices [11]. However, due to the lack of convincing experimental evidence so far, Majorana fermion still remains as elusive and its search, therefore, should expand on to uncharted routes, new systems and novel experimental designs.

The two-dimensional electron liquid (2DEL) at the LaAlO₃/SrTiO₃ interface is formed as a result of an intrinsic electronic transfer mechanism known as the polar catastrophe in which half an electronic charge is transferred from the top of the polar LaAlO₃ to the terminating TiO₂ layer on the non-polar SrTiO₃ side to avoid a charge discontinuity at the interface [12, 13]. The 2DEL becomes superconducting below 200mK [14, 15] along with large magnetic moment (~ 0.3 - $0.4 \mu_B$) aligned parallel to the interface plane [16–18]. Suggestions for the mechanism responsible for the novel ferromagnetism include a RKKY interaction [19], a double exchange process [20] and Oxygen vacancies [21] developed at the

interface during the deposition process. On the other hand, there are proposals for phonon-mediated electron-pairing [19, 20, 22] as well as unconventional superconductivity [23–25]. Another important feature of the interface is the Rashba spin-orbit interaction (SOI) which arises because of the broken mirror symmetry along perpendicular to the interface. A back-gate voltage can tune both the electron concentration and the Rashba SOI and therefore can drive a superconductor-insulator transition [26, 27] making the system a potential candidate for novel electronic devices [28].

Here we show that a magnetic field, applied perpendicular to the interface plane, can induce topological superconductivity that harbours gapless edge states and MBS at the core of a vortex. The intrinsic in-plane magnetization favours a finite momentum pairing and, therefore, weakens the topological superconducting phase. We show that by tuning the Rashba SOI (*i.e.* the back-gate voltage) the topological superconducting phase can be stabilized against the deterrent effect of the in-plane magnetization. We study the in-gap excitations and find that the zero-energy MBS located at the vortex-core is accompanied by low-energy particle-hole symmetric in-gap states of electronic origin. We study the effect of non-magnetic disorder on the low-energy excitations and observe that the MBS vanishes with moderate disorder. We propose an experimental set-up where the existence of MBS can be tested experimentally and discuss about some future directions.

The large Rashba spin-orbit interaction (RSOI), arising from the broken inversion symmetry along the \hat{z} -direction, converts the s -wave superconductivity into an effective $p_x \pm ip_y$ one. The in-plane magnetization h_x introduces asymmetry in the two-sheeted Fermi surface leading to finite-momentum pairing of electrons [29]. The main idea to get a topological superconductivity in two-dimensional s -wave superconductor with RSOI [30] is to apply a large perpendicular Zeeman field h_z to essentially remove one of the helicities of the RSOI-induced $p_x \pm ip_y$ states. One has to circumvent the deterrent effect of the in-plane magnetization to stabilize topological

* nmohanta@phy.iitkgp.ernet.in

superconductivity in this system.

In the present work, we predict that regardless of the asymmetry around the Γ -point in the Fermi surface, the single species $p_x + ip_y$ superconductivity still harbours a single MBS at the core of a vortex. We show that the tunable RSOI competes with the in-plane magnetization and restores the topological phase. However, we find that the excitation at the vortex core is highly sensitive to non-magnetic disorder; even a moderate disorder can destroy the MBS as the magnetization breaks time-reversal symmetry explicitly. As the interface in LAO/STO possesses intrinsic disorders like Oxygen vacancies, developed during the deposition process, it is indeed quite challenging to detect a Majorana fermion here. Some remedies and possible experimental requirements for realizing the MBS in this system are discussed.

II. MODEL FOR INTERFACE 2DEL

The electrons in the 2DEL occupy the three t_{2g} -bands (*viz.* d_{xy} , d_{yz} and d_{xz}) of Ti atoms in the terminating TiO_2 plane giving rise to a quarter-filled ground state. Excess electrons supplied by the Oxygen vacancies or the back-gating accumulate on the next TiO_2 layer below the interface. Electrons in the d_{xy} band are mostly localized at the interface sites due to Coulomb correlation. The electrons in the itinerant bands, in the TiO_2 layer just below the interface couple to the localized moments via ferromagnetic exchange leading to an in-plane spin-ordering of the interface electrons. The temperature variation of the gap is found to be BCS-like, $2\Delta_0/k_B T_{gap} \approx 3.4$, where Δ_0 is the pairing-gap amplitude at $T = 0$, k_B is the Boltzmann constant and T_{gap} is the gap-closing temperature [31] (the transition to the superconducting state is of BKT-type [26]); it is therefore generally assumed that the itinerant electrons at the interface undergo conventional s -wave pairing, although there are suggestions of unconventional pairing as well [23–25]. The simple model describing the interface electrons, at the mean-field level, is

$$\mathcal{H} = \sum_{\mathbf{k}, \sigma} (\epsilon_{\mathbf{k}} - \mu) c_{\mathbf{k}\sigma}^\dagger c_{\mathbf{k}\sigma} + \alpha \sum_{\mathbf{k}, \sigma, \sigma'} [\mathbf{g}_{\mathbf{k}} \cdot \boldsymbol{\sigma}]_{\sigma, \sigma'} c_{\mathbf{k}\sigma}^\dagger c_{\mathbf{k}\sigma'} - \sum_{\mathbf{k}, \sigma, \sigma'} [h_x \sigma_x]_{\sigma, \sigma'} c_{\mathbf{k}\sigma}^\dagger c_{\mathbf{k}\sigma'} + \sum_{\mathbf{k}} (\Delta c_{\mathbf{k}\uparrow}^\dagger c_{-\mathbf{k}\downarrow}^\dagger + h.c.) \quad (1)$$

where $\epsilon_{\mathbf{k}} = -2t(\cos k_x + \cos k_y)$ is the energy band dispersion with the hopping amplitude t and chemical potential μ , $\mathbf{g}_{\mathbf{k}} = (\sin k_y, -\sin k_x)$ describes the RSOI of strength α and $\Delta = -\langle c_{\mathbf{k}\uparrow} c_{-\mathbf{k}\downarrow} \rangle$ is the pairing gap and $\boldsymbol{\sigma} = [\sigma_x, \sigma_y, \sigma_z]$ being the Pauli matrices.

III. INDUCING TOPOLOGICAL SUPERCONDUCTIVITY

The RSOI breaks the spin-degeneracy of the original bands and creates two new electronic bands while the in-plane magnetization h_x shifts the Berry curvature from

the Γ -point to P $(0, -h_x/\alpha)$ point, thus making it energetically favorable for the electrons to pair up at finite center-of-mass momentum proportional to h_x . In the diagonal basis of the Rashba Hamiltonian, one essentially obtains $p_x \pm ip_y$ pairing symmetry of the superconductivity [29]. When an external Zeeman field, perpendicular to the interface 2DEL, $\mathcal{H}_Z = -h_z \sum_{\mathbf{k}} [c_{\mathbf{k}\uparrow}^\dagger c_{\mathbf{k}\uparrow} - c_{\mathbf{k}\downarrow}^\dagger c_{\mathbf{k}\downarrow}]$ is applied, a gap is opened at the point P. The pairing amplitudes in the newly created bands, $\epsilon_{\pm}(\mathbf{k}) = \epsilon'_{\mathbf{k}} \pm \xi$ are given by

$$\Delta_{\pm\pm} = -\frac{\alpha}{2\xi} \Delta (\sin k_y \pm i \sin k_x) : \text{intradband } p\text{-wave}$$

$$\Delta_{+-} = \frac{h_z}{\xi} \Delta : \text{interband } s\text{-wave}$$

where $\xi = (\alpha^2 |\mathbf{g}_{\mathbf{k}}|^2 + h^2 - 2\alpha h_x \sin k_y)^{1/2}$, $h^2 = h_x^2 + h_z^2$ and $\epsilon'_{\mathbf{k}} = \epsilon_{\mathbf{k}} - \mu$. As shown in FIG. 1, when h_z increases beyond a critical field h_{zc} , there is only one Fermi surface (*i.e.*, one of the two helicities $p_x \pm ip_y$ is removed) and the superconductivity is transformed into a topological superconductivity.

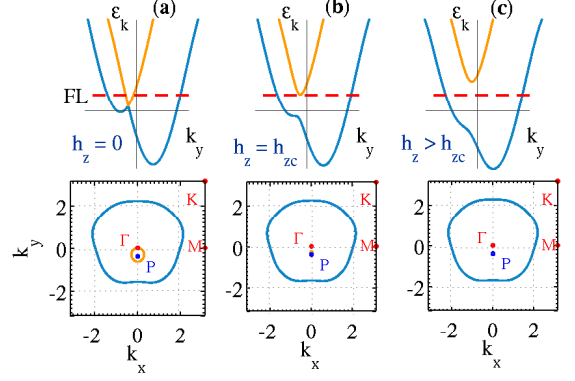


FIG. 1. (Color online) The band structure and Fermi surface: outlining the scheme of inducing topological superconductivity via external Zeeman field h_z with (a) $h_z = 0$: normal superconductivity (b) $h_z = h_{zc}$: transition point and (c) $h_z > h_{zc}$: topological superconductivity.

The effective Hamiltonian $\mathcal{H}_{eff} = \mathcal{H} + \mathcal{H}_Z$ of the system can be written in the usual Nambu basis $\Psi(\mathbf{k}) = [c_{\mathbf{k}\uparrow}, c_{\mathbf{k}\downarrow}, c_{-\mathbf{k}\downarrow}^\dagger, -c_{-\mathbf{k}\uparrow}^\dagger]$ as

$$\begin{pmatrix} \mathcal{H}_0(\mathbf{k}) & \Delta \\ \Delta & -\sigma_y \mathcal{H}_0(\mathbf{k}) \sigma_y^* \end{pmatrix} \Psi(\mathbf{k}) = E_{\pm}(\mathbf{k}) \Psi(\mathbf{k}) \quad (2)$$

where $\mathcal{H}_0(\mathbf{k}) = \epsilon'_{\mathbf{k}} + \alpha \mathbf{g}_{\mathbf{k}} \cdot \boldsymbol{\sigma} - h_z \sigma_z - h_x \sigma_x$ and we obtain the bulk spectrum $E_{\pm}^2(\mathbf{k}) = (\epsilon'_{\mathbf{k}} + \Delta^2 + \xi^2) \pm \zeta$ where $\zeta = [\Delta^2 h_z^2 + \epsilon'_{\mathbf{k}}{}^2 \xi^2]^{1/2}$. The transition to the topological state occurs only when the gap of the bulk spectrum closes *i.e.*, when $\zeta = \epsilon'_{\mathbf{k}}{}^2 + \Delta^2 + \xi^2$. This is satisfied (with $\Delta \neq 0$) when either $\xi^2 = h_z^2$ or $\epsilon'_{\mathbf{k}}{}^2 + \Delta^2 = h_z^2$ which essentially reduces to the familiar relation $h_z = \sqrt{\Delta^2 + \mu^2}$ [9] when $h_x = 0$. As h_z increases beyond this transition point, a topologically protected excitation gap E_g (given by the minimum of $E_-(\mathbf{k})$), proportional to the Rashba coupling strength α in the limit of small h_z , is induced. Therefore, E_g keeps track of the quantum phase transition from ordinary superconductivity to topological su-

perconductivity. The phase diagrams of the system, revealing the parameter regime in which the topological superconductivity can be achieved, is shown in FIG. 2. There are two competing energy gaps, the minimum of

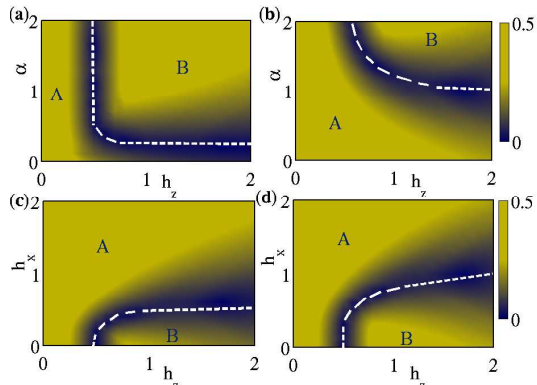


FIG. 2. (Color online) The quasi-particle excitation gap E_g in the $\alpha-h_z$ ((a) and (b)) and h_x-h_z ((c) and (d)) planes showing the quantum phase transition between the topologically trivial (region A) and non-trivial (region B) superconductors. Parameters: (a) $h_x = 0.2$, (b) $h_x = 1.0$, (c) $\alpha = 0.2$, (d) $\alpha = 1.0$ with $t = 1$, $\mu = 0$ and $\Delta = 0.5$. The dashed white lines delineate the boundary between the two phases.

which tries to destroy the topological state; one is the induced bulk excitation gap at the Fermi level ($\mathbf{k} = \mathbf{k}_F$), $\Delta_{FS} = 2\Delta_-$, the other is the Zeeman gap at the point P, given by $\Delta_z = E_-(0, -h_x/\alpha)$. In addition, the in-plane magnetization, by introducing a finite-momentum pairing, weakens the topological superconductivity. However, the RSOI competes with the in-plane magnetization to restore the topological state, which is clearly visible in the phase diagram, FIG. 2. Since the RSOI in $\text{LaAlO}_3/\text{SrTiO}_3$ interface is tunable by external gate voltage [27], it can be tuned to stabilize the topological state.

IV. VORTEX CORE EXCITATIONS

The induced topological superconductivity exhibits edge states and zero-energy MBS at the core of a vortex [32]. Since Majorana fermions are essentially half an ordinary fermion, they always come in pair, generally located in different vortex-cores. A system having only one vortex, hosts the second Majorana fermion at the boundary. The topological property of the gapless excitation at the boundary is connected to the bulk topological state as a consequence of the ‘‘bulk-boundary correspondence’’. In the following we study the vortex core states by solving the following effective BdG Hamiltonian in real space.

$$\begin{aligned} \mathcal{H} = & -t' \sum_{\langle ij \rangle, \sigma} c_{i\sigma}^\dagger c_{j\sigma} - \mu \sum_{i, \sigma} c_{i\sigma}^\dagger c_{i\sigma} - \sum_{i, \sigma, \sigma'} (\mathbf{h} \cdot \boldsymbol{\sigma})_{\sigma\sigma'} c_{i\sigma}^\dagger c_{i\sigma'} \\ & - i \frac{\alpha}{2} \sum_{\langle ij \rangle, \sigma, \sigma'} (\sigma_{\sigma\sigma'} \times \hat{\mathbf{d}}_{ij})_z c_{i\sigma}^\dagger c_{j\sigma'} + \sum_i (\Delta_i c_{i\uparrow}^\dagger c_{i\downarrow}^\dagger + h.c.) \end{aligned} \quad (3)$$

where t' is the hopping amplitude of electrons on a square lattice, $\mathbf{h} = (h_x, 0, h_z)$, $\hat{\mathbf{d}}_{ij}$ is unit vector between sites i and j , and $\Delta_i = -U(c_{i\uparrow}c_{i\downarrow})$ is the onsite pairing amplitude with U , the attractive pair-potential. The Hamiltonian (3) is diagonalized via a spin-generalized Bogoliubov-Valatin transformation $\hat{c}_{i\sigma}(r_i) = \sum_{i, \sigma'} u_{n\sigma\sigma'}(r_i) \hat{\gamma}_{n\sigma'} + v_{n\sigma\sigma'}^*(r_i) \hat{\gamma}_{n\sigma'}^\dagger$, and the quasi-particle amplitudes $u_{n\sigma}(r_i)$ and $v_{n\sigma}(r_i)$ are determined by solving the BdG equations: $\mathcal{H}\phi_n(r_i) = \epsilon_n \phi_n(r_i)$ where $\phi_n = [u_{n\uparrow}(r_i), u_{n\downarrow}(r_i), v_{n\uparrow}(r_i), v_{n\downarrow}(r_i)]$. To model a vortex, we use open boundary conditions and solve self-consistently the BdG equations by taking an initial ansatz for the gap as $\Delta_j = \Delta_0 r_j e^{i\phi_j} / \sqrt{r_j^2 + 2r_c^2}$, where (r_j, ϕ_j) are the polar coordinates of site j with respect to the core at the center of the 2D plane, Δ_0 and r_c are respectively the depth and size of the vortex core. The results, presented here, are for a 40×40 system with vortex-size $r_c = 1$. For the rest of the paper, we set $\mu = 0$, $t' = 1$ and $U = 4.0$, unless explicitly specified. In FIG. 3(a), we plot the lo-

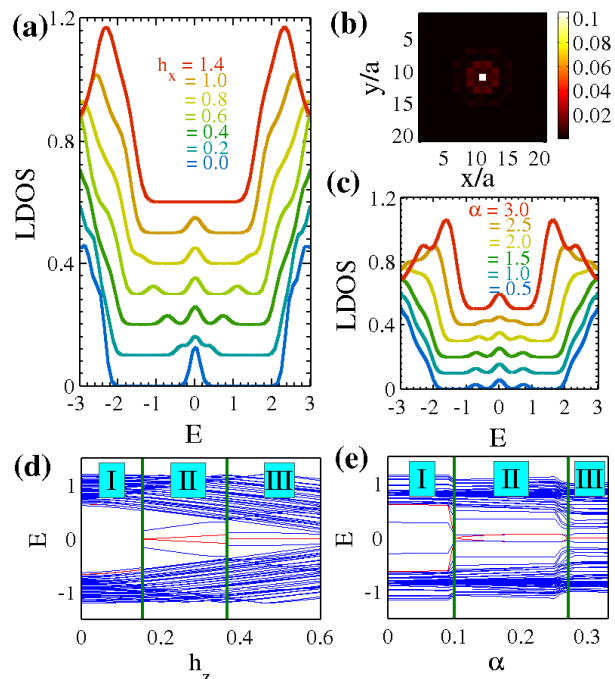


FIG. 3. (Color online) (a) The LDOS at the vortex core for in-plane fields h_x showing the MBS at zero-energy and the low-energy fermionic states for $\alpha = 1.0$ and $h_z = 1.0$. (b) Plot of the density of zero energy quasi-particles, $|u_{n\uparrow}(r_j)|^2 + |u_{n\downarrow}(r_j)|^2$, showing the vortex-core state on the 2D plane for $h_x = 0.2$, $h_z = 1.0$ and $\alpha = 1.0$ for a 25×25 system. (c) LDOS for various α with constant $h_x = 0.2$ and $h_z = 1.0$. (d)-(e) Quasi-particle spectra as a function of h_z ($\alpha = 0.2$, $h_x = 0.1$ and $U = 1$) and α ($h_z = 0.6$, $h_x = 0.2$ and $U = 1$) delineating three regions - (I) normal superconductivity, (II) normal superconductivity with magnetized vortex and (III) topological superconductivity with a Majorana BS (the red lines at zero bias).

cal density of states (LDOS) at the vortex core, given by $\rho(\epsilon, r_i) = \frac{1}{N} \sum_{n, \sigma} [|u_{n\sigma}(r_i)|^2 \delta(\epsilon - \epsilon_n) + |v_{n\sigma}(r_i)|^2 \delta(\epsilon + \epsilon_n)]$

for various in-plane field h_x , N being the total number of lattice sites. Evidently, the zero-bias Majorana mode is accompanied by other low-energy vortex-bound-states which generally appear at a vortex core in conventional superconductors and are known as the Caroli-de Gennes Matricon states [33]. These states exist in both the normal and topological superconducting phase. With increasing h_x , the fermionic states move away and mix with the bulk bands and the MBS vanishes suddenly as h_x reaches the critical value for transition to the trivial superconducting state. The Majorana excitation at the vortex core is shown in FIG. 3(b). As shown in FIG. 3(c), the bulk band-gap reduces slowly with increasing α and the low-energy fermionic excitations merge with the MBS. Remarkably, similar features of the LDOS, for various gate voltages, have been seen in the tunneling spectra obtained at 50 mK using Au-gated LAO/STO tunnel device [34]. FIG. 3(d)-(e) show three regimes: regimes I, II and III are all superconducting: region II has a magnetized vortex and only region III has non-trivial superconductivity and the Majorana modes (two red lines at zero energy for the vortex-core and edge excitations). Region II is quite interesting as it has a zero energy fermionic excitation close to the boundary of I which arises in this trivial superconducting state from the competition between the Zeeman field that magnetizes the vortex and the superconductivity, thereby changing the vortex structure [35]. The spacing between the in-gap bound states is typically of the order of Δ^2/E_F , where Δ is the gap amplitude, E_F is the Fermi energy. In the present situation, the critical temperature of the real system is not proportional to the mean-field 'gap' we are using [31]: it is dictated primarily by the coupling between the superconducting grains and therefore much smaller (200 mK) than would otherwise appear from the gap values. In the tunneling spectrum, the position of these in-gap bound states is thus not completely determined by the real T_c (200mK). However, while tuning the perpendicular magnetic field (h_z) or the gate-voltage (*i.e.*, Rashba SOI strength α), the abrupt transition from region II to region III, in FIG.3(d)-(e), can also give rise to a stronger, unique experimental signature of Majorana bound states.

V. INFLUENCE OF DISORDER

The topological excitations are, however, quite fragile against the imperfections of the host system. The LaAlO₃/SrTiO₃ interface contains intrinsic disorder such as Oxygen vacancies, known to have significant effects on the interface electrons [21, 36]. It is, therefore, imperative to study the robustness of the MBS against non-magnetic disorder, introduced through an onsite random potential V_d in the Hamiltonian (3) by $\mathcal{H}_{dis} = V_d \sum_{i,\sigma} c_{i\sigma}^\dagger c_{i\sigma}$, where, $V_d \in [-W, W]$ uniformly. In FIG. 4, we plot the density of states $\rho(\epsilon) = \frac{1}{N} \sum_{n,r_i,\sigma} [|u_{n\sigma}(r_i)|^2 \delta(\epsilon - \epsilon_n) + |v_{n\sigma}(r_i)|^2 \delta(\epsilon + \epsilon_n)]$ for disorder realizations of various disorder strength W . The MBS is quickly destroyed

as disorder increases and other in-gap excitations appear within the bulk gap due to the defects. The MBS is, in fact, not expected to be robust against perturbations like disorder in this system since the time-reversal symmetry is already broken explicitly [37]. As shown in FIG. 4,

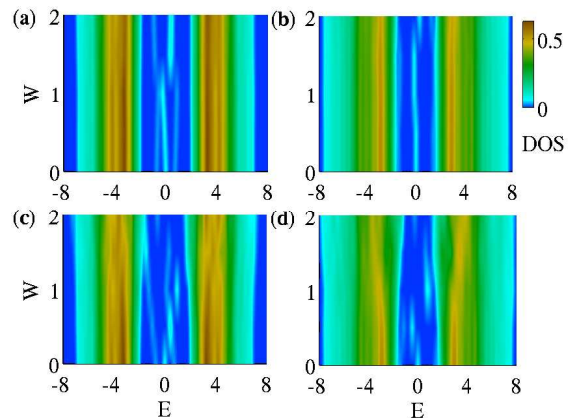


FIG. 4. (Color online) Plot of the density of states as a function of disorder strength W , revealing the behaviour of the low-energy excitations inside the bulk superconducting gap (a) $h_z = 0.5$, $h_x = 0.4$, (b) $h_z = 0.5$, $h_x = 1.0$, (c) $h_z = 1.0$, $h_x = 0.4$ and (d) $h_z = 1.0$, $h_x = 1.0$. Other parameters are same as in FIG. 3.

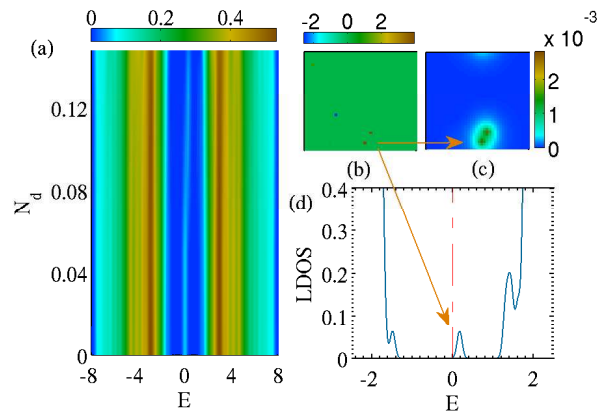


FIG. 5. (Color online) (a) Variation of the density of states with disorder concentration N_d with $W = 1$, $h_z = 0.5$, $h_x = 1.0$. (b) Disorder configuration in the 2D plane with $h_z = 0.5$, $h_x = 1.0$, $N_d = 0.003$ and $W = 2$. (c) and (d) are respectively the density of quasi-particle *i.e.* $|u_{n\uparrow}(r_j)|^2 + |u_{n\downarrow}(r_j)|^2$ and the LDOS at the defect site indicated by the arrow. Other parameters are same as in FIG. 3.

the vulnerability of the zero-energy MBS is worse in presence of larger magnetic fields. In other words, the MBS survives against larger strength of disorder when h_z is smaller (provided, h_z should always be greater than the critical value h_{zc} to ensure topological regime). In the present system, the degree of vulnerability is severe due to the in-plane magnetization which, in reality, weakens the topological state. Hence the low-energy excitations

are destroyed even when there is a finite superconducting gap. In FIG. 4, we show a situation where disorder of random strength (up to W) is present at all sites. We also consider a diluted situation by putting disorder at some random sites. FIG. 5(a) describes how the low-energy in-gap excitations are affected as the disorder concentration (N_d) is varied. We find that the results are not different qualitatively from that in FIG. 4. The zero-energy Majorana excitation remains unaffected unless a defect potential appears exactly at the vortex-core and, as in FIG. 4, new states appear within the bulk-gap. To check where these defect-induced states are localized, we plot, in FIG. 5, the quasi-particle density and LDOS spectra at a defect site. We find that, as reported previously [38], the new in-gap states are actually located at the defect sites. Therefore in the tunneling conductance measurement, getting an excitation at zero-energy does not necessarily confirm a Majorana particle. One has to be very careful in disentangling the Majorana fermion from defect induced states or Andreev bound states [39].

VI. EXPERIMENTAL ASPECTS

For the experimental realization of topological superconductivity and MBS in the interface 2DEL, an external Zeeman field h_z is required. This can be achieved by mounting the $\text{LaAlO}_3/\text{SrTiO}_3$ interface on top of a ferromagnetic insulator whose spins are aligned to the \hat{z} -direction, as shown in FIG. 6. The two major obstacles towards a realization of the topological state however, are (i) the intrinsic in-plane magnetization and (ii) the intrinsic defects. To stabilize the topological state,

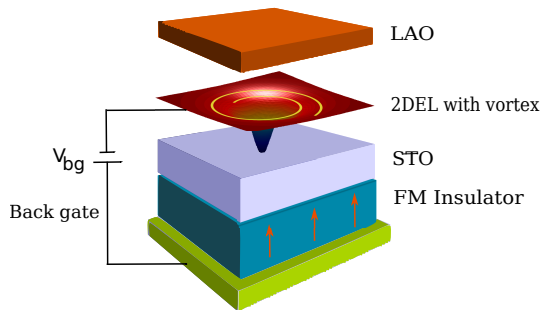


FIG. 6. (Color online) Schematic picture of the proposed setup for realization of MBS in $\text{LaAlO}_3/\text{SrTiO}_3$ interface.

the effect of the in-plane magnetization can be partially

offset by tuning the RSOI via the gate voltage. To reduce the laser-induced defects (in pulsed laser deposition method) and intrinsic disorder such as the Oxygen vacancies, molecular beam epitaxy techniques are used instead. Ozone may be used as oxidant instead of Oxygen during the annealing process as suggested by Warusawithana *et al.* [40]. High resolution scanning tunneling microscopy (STM) or point-contact spectroscopy may identify a single MBS at the vortex core. Typical experimental resolution in the tunneling experiments is about $2\mu\text{V}$ and should be sufficient to identify the zero-bias peak of the Majorana BS from the nearby excitations. Though the mean-field gap is known to be a gross over-estimation, a rescaling of the gap in FIG. 3(c) on to the experimentally observed gap, about $80\mu\text{V}$, gives a value of the resolution-limit about $13\mu\text{V}$, close to the experimental values ($\sim 9.5\mu\text{V}$) observed [34]. It is worth mentioning that the usual temperature range, in which the thermal fluctuation is small for the detection of the MBS, is less than 100 mK [7, 10] which is far below the Curie temperature (200 mK) of this interface superconductivity.

Recently, it has been shown that superconductivity is possible in quasi-1D structures, grown at the $\text{LaAlO}_3/\text{SrTiO}_3$ interface [41, 42] and may support Majorana zero modes at the ends of such quantum wires [43]. These are the steps towards developing qubits, using this interface, which is to be used as the building blocks of a topological quantum simulator.

VII. CONCLUSION

In summary, we have shown that topological superconductivity hosting Majorana fermions can be realized in the two-dimensional metallic interface of LaAlO_3 and SrTiO_3 under the right conditions. The phase diagrams show that an additional Zeeman field with large RSOI is required to achieve a stable topological superconductivity. However, non-magnetic disorder such as Oxygen vacancies are detrimental to the topological excitations. An experimental design likely to produce conditions conducive to observing Majorana excitations is proposed.

VIII. ACKNOWLEDGEMENTS

The authors thank C. Richter for sending his unpublished data and noticing the similarity with FIG. 3. NM thanks J. Mannhart for useful discussions.

-
- [1] J. Alicea, Y. Oreg, G. Refael, F. von Oppen, and M. P. A. Fisher, *Nat Phys* **7**, 412 (2011).
 - [2] D. M. Lee, *Rev. Mod. Phys.* **69**, 645 (1997).
 - [3] K. Ishida *et al.*, *Nature* **396**, 658 (1998).

- [4] G. Moore and N. Read, *Nuclear Physics B* **360**, 362 (1991).
- [5] Y. Oreg, G. Refael, and F. von Oppen, *Phys. Rev. Lett.* **105**, 177002 (2010).

- [6] R. M. Lutchyn, J. D. Sau, and S. Das Sarma, Phys. Rev. Lett. **105**, 077001 (2010).
- [7] V. Mourik *et al.*, Science **336**, 1003 (2012).
- [8] L. Fu and C. L. Kane, Phys. Rev. Lett. **100**, 096407 (2008).
- [9] J. Alicea, Phys. Rev. B **81**, 125318 (2010).
- [10] A. Das *et al.*, Nat Phys **8**, 887 (2012).
- [11] C. Zhang, S. Tewari, R. M. Lutchyn, and S. Das Sarma, Phys. Rev. Lett. **101**, 160401 (2008).
- [12] A. Ohtomo and H. Y. Hwang, Nature **427**, 423 (2004).
- [13] N. Nakagawa, H. Y. Hwang, and D. A. Muller, Nat Mater **5**, 204 (2006).
- [14] N. Reyren *et al.*, Science **317**, 1196 (2007).
- [15] S. Gariglio, N. Reyren, A. D. Caviglia, and J.-M. Triscone, J. Phys.: Condens. Matter **21**, 164213 (2009).
- [16] L. Li, C. Richter, J. Mannhart, and R. C. Ashoori, Nat Phys **7**, 762 (2011).
- [17] J. A. Bert *et al.*, Nat Phys **7**, 767 (2011).
- [18] D. A. Dikin *et al.*, Phys. Rev. Lett. **107**, 056802 (2011).
- [19] K. Michaeli, A. C. Potter, and P. A. Lee, Phys. Rev. Lett. **108**, 117003 (2012).
- [20] S. Banerjee, O. Erten, and M. Randeria, Nat Phys **9**, 626 (2013), Letter.
- [21] N. Pavlenko, T. Kopp, E. Y. Tsymbal, J. Mannhart, and G. A. Sawatzky, Phys. Rev. B **86**, 064431 (2012).
- [22] S. N. Klimin, J. Tempere, J. T. Devreese, and D. van der Marel, Phys. Rev. B **89**, 184514 (2014).
- [23] M. S. Scheurer and J. Schmalian, arxiv e-prints 1404.4039 (2014).
- [24] L. Fidkowski, H.-C. Jiang, R. M. Lutchyn, and C. Nayak, Phys. Rev. B **87**, 014436 (2013).
- [25] S. Caprara *et al.*, arxiv e-prints 1304.2970 (2013).
- [26] A. D. Caviglia *et al.*, Nature **456**, 624 (2008).
- [27] A. D. Caviglia *et al.*, Phys. Rev. Lett. **104**, 126803 (2010).
- [28] J. Mannhart and D. G. Schlom, Science **327**, 1607 (2010).
- [29] N. Mohanta and A. Taraphder, Journal of Physics: Condensed Matter **26**, 025705 (2014).
- [30] S. Fujimoto, Phys. Rev. B **77**, 220501 (2008).
- [31] C. Richter *et al.*, Nature **502**, 528 (2013), Letter.
- [32] Y. Nagai, H. Nakamura, and M. Machida, J. Phys. Soc. Jpn. **83**, 064703 (2014).
- [33] C. Caroli, P. D. Gennes, and J. Matricon, Physics Letters **9**, 307 (1964).
- [34] C. Richter, *Experimental Investigation of Electronic and Magnetic Properties of LaAlO₃-SrTiO₃ Interfaces*, PhD thesis, University of Augsburg, 2012.
- [35] K. Björnson and A. M. Black-Schaffer, Phys. Rev. B **88**, 024501 (2013).
- [36] N. Mohanta and A. Taraphder, Journal of Physics: Condensed Matter **26**, 215703 (2014).
- [37] A. C. Potter and P. A. Lee, Phys. Rev. B **83**, 184520 (2011).
- [38] Y. Nagai, Y. Ota, and M. Machida, arxiv e-prints 1407.1125 (2014).
- [39] T. D. Stanescu and S. Tewari, Phys. Rev. B **87**, 140504 (2013).
- [40] M. P. Warusawithana *et al.*, Nat Commun **4** (2013).
- [41] C. Cen *et al.*, arxiv e-prints 1009.2424 (2010).
- [42] J. P. Veazey *et al.*, arxiv e-prints 1210.3606 (2012).
- [43] L. Fidkowski, R. M. Lutchyn, C. Nayak, and M. P. A. Fisher, Phys. Rev. B **84**, 195436 (2011).